COBEM 2023 27TH INTERNATIONAL CONGRESS OF MECHANICAL ENGINEERING

ABCM Brazilian Society of Mechanical Sciences and Engineering
27th ABCM International Congress of Mechanical Engineering
December 04-08, 2023, Florianópolis-SC, Brazil

COB-2023-0784
ON THE DESIGN OF NONLINEAR RESONATORS TO IMPROVE THE DISPLACEMENT TRANSMISSIBILITY OF MONO-COUPLED PERIODIC ROD STRUCTURES

Felipe Alves Anezio
Paulo J. Paupitz Gonçalves
State University of São Paulo (UNESP), School of Engineering, Bauru
felipe.anezio@unesp.br
paulo.paupitz@unesp.br

Douglas Roca Santo
Leopoldo P. Rodrigues de Oliveira
University of São Paulo (USP), School of Engineering
douglas.roca@usp.br
leopro@sc.usp.br

Abstract. *The study of periodic structures is closely linked to the field of metamaterials. When elastic waves propagate through these structures, they are reshaped, resulting in frequency intervals where the waves cannot freely propagate, known as bandgaps. A key idea in this research is to model a unitary cell of the periodic structure with a non-linear resonator attachment. The resonant frequencies of a structure coupled to non-linear springs depend on the displacement levels, which can be translated into a broadening frequency range. This makes the non-linear response interesting as the effect of grading metamaterials is achieved due to the different levels each resonator vibrates. The Harmonic Balance analytical method is used to produce an approximate polynomial equation for accurately calculating frequency response functions (FRFs). Comparisons were made with numerical solutions, integrating displacements using the Runge-Kutta method and implementing a finite element model. The displacement transmissibility shows an increase in the bandgap region, where three possible responses also occurred, compared to the purely linear resonator. The non-linear stiffness associated with the added vibration absorber changed the dynamic behavior of the device, generating some advantages at lower frequencies, allowing for a reduction in mass. These findings open interesting perspectives on vibration control in periodic structures connected to non-linear resonators.*

Keywords: *periodic structures, resonant metamaterial, non-linear analysis*

1. INTRODUCTION

Traditional metamaterials utilize the theory of Bragg scattering. The lattices are created such that when the waves reflect off the structure, they destructively interfere with each other. In order for the Bragg scattering mechanism to work, the periodic length of the material must be of similar length as the wavelength (Reichl and Inman, 2017). When periodic structures have point defects or linear defects, elastic waves within the band gap will be restricted to the point defect or only propagate along the linear defects. The property of elastic wave band gaps gives broad application potential in noise reduction and vibration attenuation, such as passive sound insulation and vibration attenuation (Wen *et al.*, 2008).

In metamaterials with local resonators, the low frequency bandgap when compared to the Bragg mechanism was explained by the negative effective mass density through equivalent discrete mass-spring systems. Band gaps, therefore, may be due to Bragg effects (Kushwaha *et al.*, 1993) or local resonance effects (Hussein *et al.*, 2014; Huang *et al.*, 2016). An acoustic (or elastic) metamaterial, is also (usually) a periodic material except it has the added feature of exhibiting local resonance, or possibly other traits, that can give rise to dynamic behavior, such as negative refraction and negative group velocity. Resonator effects generate band gaps at lower frequencies (Hussein *et al.*, 2014; Reichl and Inman, 2017).

Recently, Pai (2010) proposed metamaterial of a uniform isotropic beam with many small spring-mass-damper subsystems integrated at separated locations along the beam to act as vibration absorbers. For a unit cell of an infinite metamaterial beam, governing equations are derived using the extended Hamilton principle. This local mechanical resonance can be used to design acoustic metamaterials with negative effective mass and stiffness. The suspension concept uses the incident elastic wave to resonate the absorption devices in the metamaterial and controlled wave control. Recent work, Zhu *et al.* (2014) the locally resonant (LR) mechanism could be easily tuned through proper microstructure design, and low-frequency vibration energy could be quickly attenuated within only a small amount of the periodic microstructures. Zhu *et al.* (2014) focuses on the design of a beam metastructure composed of oscillators that is developed for wideband

vibration attenuation, utilizing the individual *bandgaps*. What is interesting in some of these works is that the new gaps produced by appended elements coexisted with the Bragg *bandgap* due to the systematic periodicity of metamaterials.

The issue, however, is that band gaps are likely to occur at frequencies higher than those often encountered in engineering structural vibration problems (Zhu *et al.*, 2014). On the other hand, nonlinear devices possess additional interesting properties which make them useful at low frequencies. The key idea is that the resonance frequencies of a structure coupled to an array of nonlinear devices depend on the displacement levels, and as such, they can be shifted to high frequencies (Santo *et al.*, 2020).

There exist several analytical methods to analyze the dynamic behavior of discrete nonlinear systems, the method of multiple scales, the averaging methods and the harmonic balance method (Brennan *et al.*, 2008; Holmes and Holmes, 1981; Kevorkian and Cole, 2013). These methods mainly focus on assessing the effect of the nonlinearity on the (first) natural frequency of the systems. They are often based on the Duffing oscillator equation, which is well suited to represent stiffness nonlinearities in typical engineering (Kovacic and Brennan, 2011; Nayfeh and Mook, 2008; Carrella *et al.*, 2007; Gao *et al.*, 2019; Santo *et al.*, 2018).

2. METHODOLOGY

The system shown in Fig. 1 consists rod comprised of N identical cells where longitudinal vibration is considered. The n-th cell is illustrated in detail, where the rod has uniform cross section area A, Young's Modulus E, mass density ρ and cell total length $2l$. At it's middle point, a resonant system consisting of a mass m and nonlinear spring characterized by spring constants s_1 and s_3 (discussed later in section 2.1). The amplitude of complex displacements at both ends of the rod are defined as U_1 (left) and U_3 (right) and a harmonic force amplitude F_1 is applied at the left hand side of the rod. The middle point displacement is defined by U_2 and the mass attached thought the nonlinear spring has displacement amplitude defined by Y_a.

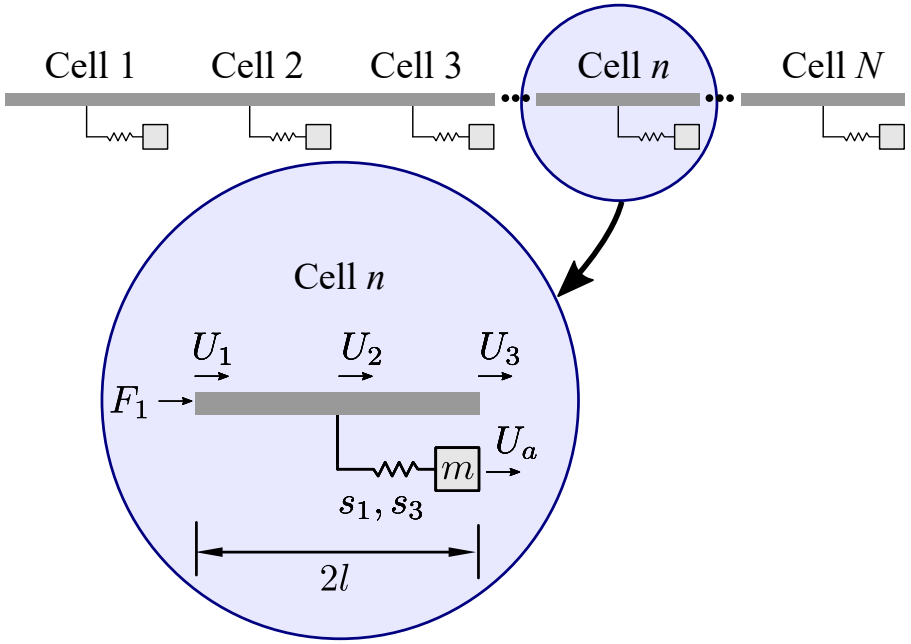

Figure 1. A rod system with N cells with resonators attached. The n-th cell is shown in detail of the figure.

According to (Gonçalves *et al.*, 2021) the properties of the whole structure can be determined from the transmissibility of a single element. If the element is symmetric, then the expressions describing the stop-band are particularly simple.

2.1 Polinomial method

In the case the spring is coupled to the cell in position U_2. The spring restoring force is represented.

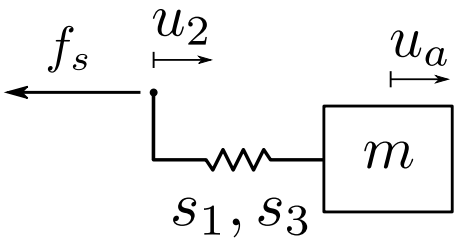

Figure 2. Schematic diagram of a non-linear absorber attached at the right end and its restoring force f_s.

For this work, it is assumed that the spring (*Duffing*) is governed by a cubic function (Kovacic and Brennan, 2011; Kargarnovin *et al.*, 2005; Inman, 2002; Santo *et al.*, 2020), which links the restoring force $f_s = f_s(t)$ to the displacement $u = u(t)$ of the central region of the cell:

$$f_s = s_1 z \pm s_3 z^3, \tag{1}$$

where z is the relative deformation, s_1 and s_3 are the linear and non-linear coefficients of the spring, respectively. The examples that follow in Fig. 3 show the behavior of the magnitude of the spring restoration force, for two non-linear stiffness coefficients: positive (*hardening* - blue line) and negative (*softening* - red line).

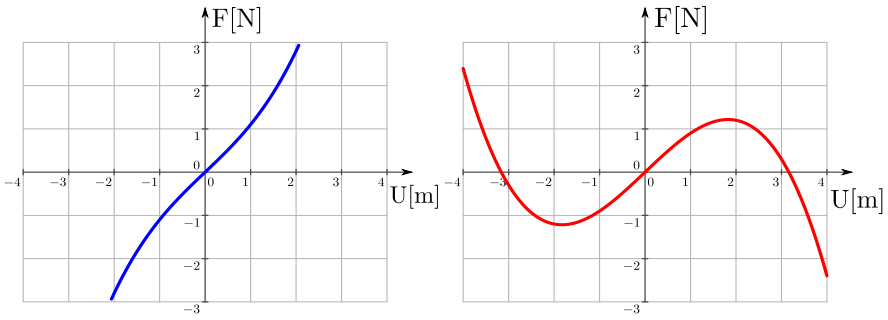

Figure 3. Spring restoring force against displacement, when $s_1 = 1$ N/m and $s_3 = 0,1$ N/m^{-3} (blue line) and when $s_1 = 1$ N/m and $s_3 = -0,1$ N/m^{-3} (red line).

It is shown that for the case of *hardening* stiffness the spring is stiffening with increasing deformation. However, for the case of the spring *softening* the equivalent stiffness is becoming negative when the magnitude of the displacement exceeds a certain value, that is, the system becomes unstable. For small values of displacements, an equivalent linear stiffness can be defined, represented by the slope of the curves shown.

Assuming harmonic force with frequency ω, this means, $f(t) = F\cos(\omega t)$ and that the displacement follows this (harmonic) pattern related to the input force. The displacement then can be expressed by $u(t) = U\cos(\omega t)$, by first-order Fourier series expansion (Mickens, 2001). As a result, Eq. 2 can be rewritten as follows:

$$F_s\cos(\omega t) = -\omega^2 m\cos(\omega t)Z + s_1 Z\cos(\omega t) \pm s_3 Z^3\cos^3(\omega t), \tag{2}$$

where z is the relative displacemente, $z = u_2 - u_a$. For the equivalent stiffness of the spring, an expression corresponding to the frequency was obtained with the trigonometric relation $\cos^3(\omega t) = 3/4\cos(\omega t) + 1/4\cos(3\omega t)$ and canceling the term associated with the third harmonic (3ω). Therefore, the equivalent stiffness of the non-linear ressonator $D(Z)$ can be expressed in terms of these parameters.

$$D(Z) = \frac{F_s}{Z} = -\omega^2 m + s_1 \pm \frac{3}{4}s_3 Z^2, \tag{3}$$

Note that the equivalent nonlinear stiffness $D(Z)$ is a function of the displacement amplitude, which depends on the point at which the spring was attached.

The dynamic stiffness matrix of the unit cell can be obtained. The stiffness elements D_1 and D_2 are part of the matrix for the member. For this case they are defined as $D_1 = EAk\cot(kl)$ and $D_2 = -EAk/\sin(kl)$:

$$\begin{bmatrix} D_1 & D_2 & 0 \\ D_2 & D_1 + D(Z) & D_2 \\ 0 & D_2 & D_1 \end{bmatrix} \begin{Bmatrix} U_1 \\ U_2 \\ U_3 \end{Bmatrix} = \begin{Bmatrix} F_1 \\ 0 \\ 0 \end{Bmatrix}, \tag{4}$$

where $D(Z)$ is the equivalent stiffness of the ressonator, linear and non-linear, A the cross-sectional area of the bar, E Young's modulus and k weve number. The matrix results in the polynomial linked to the position in which you want to evaluate the response:

$$a_3 U^3 + a_1 U + a_0 = 0, \tag{5}$$

where a_0, a_1 and a_3 are frequency-dependent coefficients. One of the main advantages of the proposed approach is that it can represent the multimode behavior (multiple resonances) of the unit cell over a wide frequency range.

2.2 Numerical Method and Finite Element Analysis

In non-linear conditions, numerical integration is often used using, for example, the Runge-Kutta method. For this, the system can be written in state space form:

$$\dot{\mathbf{y}}_1 = \mathbf{y}_2 \tag{6}$$
$$\dot{\mathbf{y}}_2 = g\left(\mathbf{y}_1, \mathbf{y}_2\right), \tag{7}$$

where $\{y_1\}$ and $\{y_2\}$ are state vectors, and $\{g\}$ is a function of the states of the system. For the bar with the resonator attached the equations of motion are described in matrix form:

$$\mathbf{M}\ddot{\mathbf{u}} + \mathbf{C}\dot{\mathbf{u}} + \mathbf{K}\mathbf{u} = \mathbf{f}(t) + \mathbf{f}_{nl}(t), \tag{8}$$

where $\mathbf{M}$ is the mass matrix, $\mathbf{K}$ is the stiffness matrix, and $\mathbf{C}$ is the general damping matrix for the bar. The vector $\mathbf{f}$ represents the external forces and $\mathbf{f}_{nl}$ the non-linear behavior of the ressonator. These general matrices can be obtained considering the number of elements. As the function is non-linear, the simulations were carried out in the time domain, obtaining the maximum displacement levels. Considering the formulation shown, we rewrite the motion equations in state space form.

$$\dot{\mathbf{y}} = \mathbf{A}\mathbf{u} + \mathbf{B}\,\mathbf{f} + \mathbf{B}\,\mathbf{f}_{nl}, \tag{9}$$

In this formulation $\dot{\mathbf{u}}$ represents the state vector of the system. The matrices $\mathbf{A}$ and $\mathbf{B}$ are obtained according to the number of elements considered.

$$\mathbf{A} = \begin{bmatrix} \mathbf{O} & \mathbf{I} \\ -\mathbf{M}^{-1}\mathbf{K} & -\mathbf{M}^{-1}\mathbf{C} \end{bmatrix}, \quad \mathbf{B} = \begin{bmatrix} \mathbf{O} \\ \mathbf{M}^{-1} \end{bmatrix} \tag{10}$$

where, $\mathbf{O}$ the matrix of zeros and $\mathbf{I}$ the identity matrix, whose dimensions depend on the subdivision of elements. Numerical simulation evaluates the system response function and maximum displacement values in the time domain. These results can be integrated to represent the frequency response of the structure. In this step, the ODE45 function was used.

3. RESULTS

In Fig. 4 the absorber was tuned to oscillate at frequencies equal to π and 2π, respectively. This produced an attenuation region at the point of the original resonance of the system without the ressonator. The resonances started to stay around the point to which the absorber was tuned.

The Fig. 4 shows the response functions obtained through the polynomial method for the bar attached to a non-linear ressonator. There are frequency intervals in which more than one solution for displacement coexists, differentiated by the colors of the lines (black, blue and red lines). It was noted that the resonant frequencies generated by the non-linear ressonator could be translated to higher frequencies, which also generated gains in the low frequency range. This occurs because the highest displacement amplitudes that occur close to the system resonances are significantly influenced by the cubic displacement term due to the presence of the nonlinear spring. The slope characteristic of the curves is influenced by the type of spring stiffness, hardening or softening stiffness. This can verified by a small benefit in the transmissibility function, along with an increase in the non-linear *bandgap* range at the operating point.

The response for the relative displacement Z and for the position of the mass of the absorber U_a is shown in the Fig. 5. All resonances were influenced by the non-linear stiffness in the infinite peaks that the system presents. Several intervals where three structural displacement solutions occur can be verified.

The Finite Element Method (FEM) was used to verify the results obtained with the polynomial method. This method was able to identify the non-linear stiffness influences that occur near the resonances generated by the presence of the ressonator. The frequency range encompassing the band gap is around $kl = \pi$. In this region the absorber was tuned and the amplitudes transmitted to the end of the structure are attenuated in the resonance region. This increase is observed

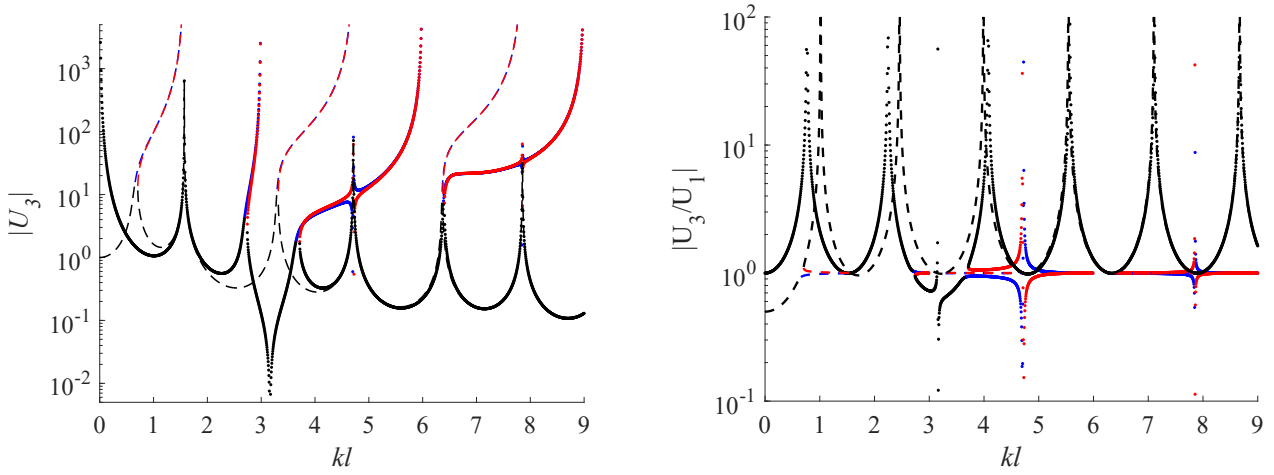

(a) (b)

Figure 4. Rod with an attached nonlinear absorber, dashed line represents the nonlinear spring system case and solid line represents the non-linear absorber case. Blue and red lines represent that there is more than one displacement solution in these regions: (a) displacement referring to position U_3, (b) transmissibility function U_3/U_1.

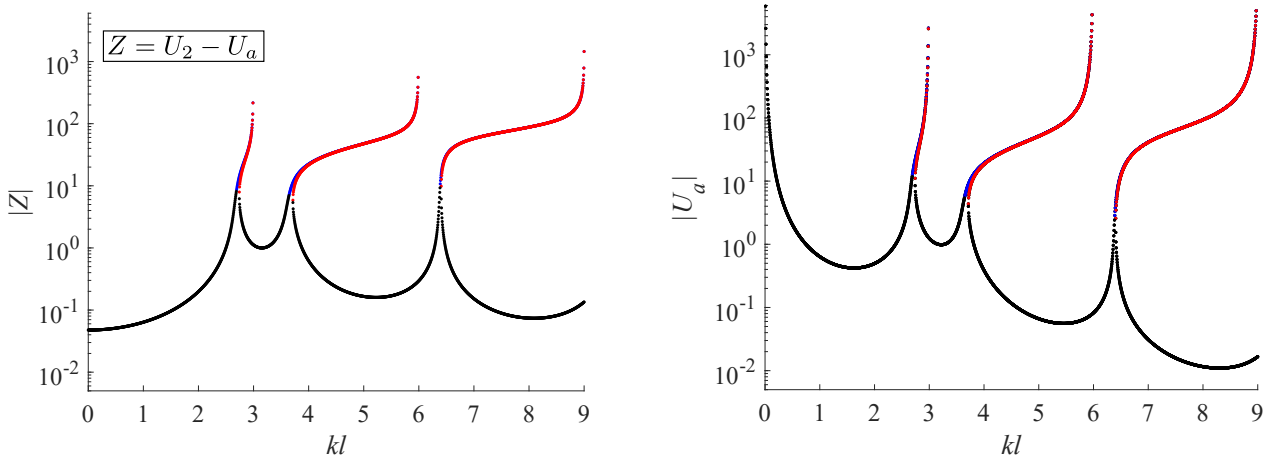

(a) (b)

Figure 5. Rod with an attached nonlinear absorber: (a) relative displacement Z, (b) resonator mass displacement U_a.

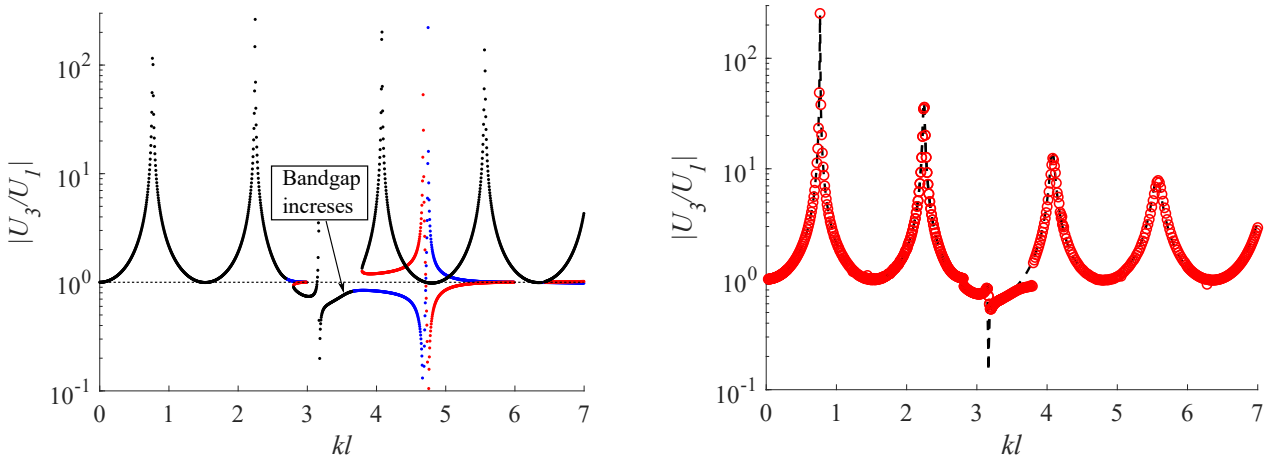

(a) (b)

Figure 6. Rod with an attached nonlinear absorber: (a) transmissibility polynomial method, (b) transmissibility Finite Element Method analysis. The dashed line represents the linear case and the red circles represent the non-linear response obtained by the FEM

when comparing the response of the structure attached to the nonlinear spring without the presence of the absorber, see the Fig. 4(b).

The Finite Element Method was able to identify the small increase in *bandgap* width due to the presence of the non-linear absorber

The implementation of the nonlinear Finite Element Method can also open the possibility of evaluating more complex periodic structures, increasing the number of local nonlinearities. In the analysis obtained by the FEM, the resonance peak around $kl = \pi$ is not identified because the numerical method is not capable of integrating the three amplitude solutions. The displacements generated consider only the amplitude points of the first solution by numerical integration. Not being able to define unstable system response.

Note that, neither the valleys nor the peaks in the transmissibility curves are affected by the nonlinearity, since these frequencies are related to low amplitude displacements.

4. CONCLUSIONS

The harmonic response of a unit cell subjected to longitudinal vibration was investigated using both polynomial and numerical methods. The polynomial method uses closed-form solutions of the system equation of motion to predict the nonlinear behavior of periodic systems in a wide frequency range. This method was found to be very efficient for modeling the dynamic response of the unit cell, and it can be used to identify regions where more than one displacement solution coexists.

Numerical simulations using the Runge-Kutta method were performed to validate the results of the polynomial method. These simulations showed that the absorber can create control intervals at low frequency where the vibration levels remain attenuated. The nonlinear spring also had a benefit in the transmissibility curve, which is the region where three possible responses occur.

The results obtained in this study may be interesting for the research area of nonlinear metamaterials. This is because the methods used in this study can be used to predict the nonlinear behavior of periodic systems in a wide frequency range. This information could be used to design metamaterials with specific nonlinear properties.

5. REFERENCES

Brennan, M., Kovacic, I., Carrella, A. and Waters, T., 2008. "On the jump-up and jump-down frequencies of the duffing oscillator". *Journal of Sound and Vibration*, Vol. 318, pp. 1250–1261.

Carrella, A., Brennan, M. and Waters, T., 2007. "Static analysis of a passive vibration isolator with quasi-zero-stiffness characteristic". *Journal of sound and vibration*, Vol. 301, pp. 678–689.

Gao, F., Wu, Z., Li, F. and Zhang, C., 2019. "Numerical and experimental analysis of the vibration and band-gap properties of elastic beams with periodically variable cross sections". *Waves in Random and Complex Media*, Vol. 29, pp. 299–316.

Gonçalves, P., Brennan, M. and Cleante, V., 2021. "Predicting the stop-band behaviour of finite mono-coupled periodic structures from the transmissibility of a single element". *Mechanical Systems and Signal Processing*, Vol. 154, p. 107512.

Holmes, C. and Holmes, P., 1981. "Second order averaging and bifurcations to subharmonics in duffing's equation". *Journal of Sound and Vibration*, Vol. 78, pp. 161–174.

Huang, H.H., Lin, C.K. and Tan, K.T., 2016. "Attenuation of transverse waves by using a metamaterial beam with lateral local resonators". *Smart Materials and Structures*, Vol. 25, p. 085027.

Hussein, M.I., Leamy, M.J. and Ruzzene, M., 2014. "Dynamics of phononic materials and structures: Historical origins, recent progress, and future outlook". *Applied Mechanics Reviews*, Vol. 66, p. 040802.

Inman, D.J., 2002. "Nonlinearity in structural dynamics: detection, identification and modelling". *Proceedings of the Institution of Mechanical Engineers*, Vol. 216, p. 383.

Kargarnovin, M., Younesian, D., Thompson, D. and Jones, C., 2005. "Response of beams on nonlinear viscoelastic foundations to harmonic moving loads". *Computers & Structures*, Vol. 83, pp. 1865–1877.

Kevorkian, J. and Cole, J.D., 2013. *Perturbation methods in applied mathematics*. Springer Science & Business Media.

Kovacic, I. and Brennan, M.J., 2011. *The Duffing equation: nonlinear oscillators and their behaviour*. John Wiley & Sons.

Kushwaha, M.S., Halevi, P., Dobrzynski, L. and Djafari-Rouhani, B., 1993. "Acoustic band structure of periodic elastic composites". *Physical review letters*, Vol. 71, p. 2022.

Mickens, R., 2001. "Mathematical and numerical study of the duffing-harmonic oscillator". *Journal of Sound Vibration*, Vol. 244, pp. 563–567.

Nayfeh, A.H. and Mook, D.T., 2008. *Nonlinear oscillations*. John Wiley & Sons.

Pai, P.F., 2010. "Metamaterial-based broadband elastic wave absorber". *Journal of intelligent material systems and structures*, Vol. 21, pp. 517–528.

Reichl, K.K. and Inman, D.J., 2017. "Lumped mass model of a 1d metastructure for vibration suppression with no additional mass". *Journal of Sound and Vibration*, Vol. 403, pp. 75–89.

Santo, D.R., Mencik, J.M. and Gonçalves, P.J.P., 2020. "On the multi-mode behavior of vibrating rods attached to nonlinear springs". *Nonlinear Dynamics*, Vol. 100, pp. 2187–2203.

Santo, D., Balthazar, J., Tusset, A., Piccirilo, V., Brasil, R. and Silveira, M., 2018. "On nonlinear horizontal dynamics and vibrations control for high-speed elevators". *Journal of Vibration and Control*, Vol. 24, pp. 825–838.

Wen, J., Wang, G., Yu, D., Zhao, H., Liu, Y. and Wen, X., 2008. "Study on the vibration band gap and vibration attenuation property of phononic crystals". *Science in China Series E: Technological Sciences*, Vol. 51, pp. 85–99.

Zhu, R., Liu, X., Hu, G., Sun, C. and Huang, G., 2014. "A chiral elastic metamaterial beam for broadband vibration suppression". *Journal of Sound and Vibration*, Vol. 333, pp. 2759–2773.

6. RESPONSIBILITY NOTICE

The authors are the only responsibles for the printed material included in this paper.